11. Chen GQ, et al. (1996) In vitro studies on cellular and molecular mechanisms of arsenic trioxide (As2O3) in the treatment of acute promyelocytic leukemia: As2O3 induces NB4 cell apoptosis with downregulation of Bcl-2 expression and modulation of PML-RAR alpha/PML proteins. *Blood* 88(3):1052–1061.
12. Gurrieri C, et al. (2004) Loss of the tumor suppressor PML in human cancers of multiple histologic origins. *J Natl Cancer Inst* 96(4):269–279.
13. Ito K, et al. (2008) PML targeting eradicates quiescent leukaemia-initiating cells. *Nature* 453(7198):1072–1078.
14. Trotman LC, et al. (2006) Identification of a tumour suppressor network opposing nuclear Akt function. *Nature* 441(7092):523–527.
15. Bernardi R, et al. (2004) PML regulates p53 stability by sequestering Mdm2 to the nucleolus. *Nat Cell Biol* 6(7):665–672.
16. Vallian S, et al. (1997) Transcriptional repression by the promyelocytic leukemia protein, PML. *Exp Cell Res* 237(2):371–382.
17. Guo D, et al. (2009) EGFR signaling through an Akt-SREBP-1-dependent, rapamycin-resistant pathway sensitizes glioblastomas to antilipogenic therapy. *Sci Signal* 2(101): ra82.
18. Lu KV, et al. (2009) Fyn and SRC are effectors of oncogenic epidermal growth factor receptor signaling in glioblastoma patients. *Cancer Res* 69(17):6889–6898.
19. Aronson SM (1994) Arsenic and old myths. *R I Med* 77(7):233–234.
20. Mathews V, et al. (2006) Single-agent arsenic trioxide in the treatment of newly diagnosed acute promyelocytic leukemia: Durable remissions with minimal toxicity. *Blood* 107(7):2627–2632.
21. Soignet SL, et al. (1998) Complete remission after treatment of acute promyelocytic leukemia with arsenic trioxide. *N Engl J Med* 339(19):1341–1348.
22. Lallemand-Breitenbach V, et al. (2001) Role of promyelocytic leukemia (PML) sumolation in nuclear body formation, 11S proteasome recruitment, and As2O3-induced PML or PML/retinoic acid receptor alpha degradation. *J Exp Med* 193(12):1361–1371.
23. de Thé H, Chen Z (2010) Acute promyelocytic leukaemia: Novel insights into the mechanisms of cure. *Nat Rev Cancer* 10(11):775–783.
24. Lallemand-Breitenbach V, Zhu J, Chen Z, de Thé H (2012) Curing APL through PML/RARA degradation by As2O3. *Trends Mol Med* 18(1):36–42.
25. Zhao S, Tsuchida T, Kawakami K, Shi C, Kawamoto K (2002) Effect of As2O3 on cell cycle progression and cyclins D1 and B1 expression in two glioblastoma cell lines differing in p53 status. *Int J Oncol* 21(1):49–55.
26. Mellinghoff IK, et al. (2005) Molecular determinants of the response of glioblastomas to EGFR kinase inhibitors. *N Engl J Med* 353(19):2012–2024.
27. Gambacorta M, et al. (1996) Heterogeneous nuclear expression of the promyelocytic leukemia (PML) protein in normal and neoplastic human tissues. *Am J Pathol* 149(6): 2023–2035.
28. Bernardi R, et al. (2011) Pml represses tumour progression through inhibition of mTOR. *EMBO Mol Med* 3(5):249–257.
29. Scaglioni PP, et al. (2012) Translation-dependent mechanisms lead to PML upregulation and mediate oncogenic K-RAS-induced cellular senescence. *EMBO Mol Med* 4(7):594–602.
30. Ito K, et al. (2012) A PML–PPAR-δ pathway for fatty acid oxidation regulates hematopoietic stem cell maintenance. *Nat Med* 18(9):1350–1358.
31. Carracedo A, et al. (2012) A metabolic prosurvival role for PML in breast cancer. *J Clin Invest* 122(9):3088–3100.
32. Cvrljevic AN, et al. (2011) Activation of Src induces mitochondrial localisation of de2-7EGFR (EGFRvIII) in glioma cells: Implications for glucose metabolism. *J Cell Sci* 124(Pt 17):2938–2950.
33. Wang MY, et al. (2006) Mammalian target of rapamycin inhibition promotes response to epidermal growth factor receptor kinase inhibitors in PTEN-deficient and PTEN-intact glioblastoma cells. *Cancer Res* 66(16):7864–7869.
34. Zhang XW, et al. (2010) Arsenic trioxide controls the fate of the PML-RARalpha oncoprotein by directly binding PML. *Science* 328(5975):240–243.
35. Grimm SA, et al. (2012) Phase I study of arsenic trioxide and temozolomide in combination with radiation therapy in patients with malignant gliomas. *J Neurooncol* 110(2):237–243.
36. Geschwind DH, et al. (2001) A genetic analysis of neural progenitor differentiation. *Neuron* 29(2):325–339.
37. Nguyen LA, et al. (2005) Physical and functional link of the leukemia-associated factors AML1 and PML. *Blood* 105(1):292–300.

MOZ increases p53 acetylation and premature senescence through its complex formation with PML

Susumu Rokudai[a], Oleg Laptenko[a], Suzzette M. Arnal[a], Yoichi Taya[b], Issay Kitabayashi[c], and Carol Prives[a,1]

[a]Department of Biological Sciences, Columbia University, New York, NY 10027; [b]Cancer Science Institute of Singapore and Department of Biochemistry, Center for Life Sciences #02-07, National University of Singapore, Singapore 117456; and [c]Molecular Oncology Division, National Cancer Center Research Institute, Chuo-ku, Tokyo 104-0045, Japan

Contributed by Carol Prives, January 18, 2013 (sent for review September 18, 2012)

Monocytic leukemia zinc finger (MOZ)/KAT6A is a MOZ, Ybf2/Sas3, Sas2, Tip60 (MYST)-type histone acetyltransferase that functions as a coactivator for acute myeloid leukemia 1 protein (AML1)- and Ets family transcription factor PU.1-dependent transcription. We previously reported that MOZ directly interacts with p53 and is essential for p53-dependent selective regulation of p21 expression. We show here that MOZ is an acetyltransferase of p53 at K120 and K382 and colocalizes with p53 in promyelocytic leukemia (PML) nuclear bodies following cellular stress. The MOZ–PML–p53 interaction enhances MOZ-mediated acetylation of p53, and this ternary complex enhances p53-dependent p21 expression. Moreover, we identified an Akt/protein kinase B recognition sequence in the PML-binding domain of MOZ protein. Akt-mediated phosphorylation of MOZ at T369 has a negative effect on complex formation between PML and MOZ. As a result of PML-mediated suppression of Akt, the increased PML–MOZ interaction enhances p21 expression and induces p53-dependent premature senescence upon forced PML expression. Our research demonstrates that MOZ controls p53 acetylation and transcriptional activity via association with PML.

protein modification | DNA damage

The p53 protein functions as a key regulator of pathways mediating cellular responses by inducing myriad target genes that regulate diverse cellular processes including cell-cycle arrest, apoptosis, and genomic stability (1–4). Regulation of p53 transcriptional activities is crucial for genotoxic stress because of the varieties of cellular responses that are mediated by p53, which, in some cases, can be mutually exclusive (e.g., arrest and apoptosis) (5). p53 has been detected in discrete nuclear speckles, known as promyelocytic leukemia nuclear bodies (PML-NBs), in which CREB binding protein (CBP)/p300, Tip60, and pRB are also found (6–8).

PML was originally identified as a *t*(15, 17) chromosomal translocation partner with the retinoic acid receptor-α (RARα) in acute promyelocytic leukemia, in which fusion genes encoding the PML-RARα fusion protein are generated (9–11). The ability of PML to interact with activators such as CBP/p300 in the nuclear body suggests that PML could modulate transcription through its ability to stabilize complexes of cofactors (12, 13). Overexpression of PML, γ-irradiation of cells, or oncogenic signals such as Ras overexpression can recruit p53 into PML-NBs (14, 15). The resulting ternary p53–PML–CBP complex then promotes the acetylation of p53 and harmonically coordinates critical tumor-suppressive functions such as apoptosis, senescence, and growth arrest (16, 17). Unlike bona fide coactivators such as CBP and p300, PML does not possess intrinsic histone acetylase activity. PML-mediated recruitment of both coactivators promotes p53 modification, such as acetylation and phosphorylation (16, 17). Acetylation levels of p53 are known to be significantly enhanced in response to stress and are involved in p53 activation and stabilization (18, 19). Given that $p300^{-/-}$ mouse embryonic fibroblasts (MEFs) retain the ability to respond to UV irradiation by stabilization of p53 and induction of p21, it is possible that other cofactors may compensate for p300 function in $p300^{-/-}$ MEFs (20).

Recent studies have shown PML to be a component of the PI3K-signaling network, negatively regulating the nuclear content of phosphorylated Akt/protein kinase B via its dephosphorylation by protein phosphatase 2A (PP2A) (21). The PI3K-Akt pathway has also been well documented to delay the p53-mediated response (22). The central role of Akt in this process is illustrated by the physical association of Akt with murine double minute 2 (MDM2), which inhibits p21 expression through its phosphorylation and activation of MDM2 and subsequent MDM2-mediated ubiquitination of p53 (23, 24). Recent studies suggest that Mdm2 mediates transcriptional repression by forming a protein complex with p53 on the promoter of specific p53-responsive genes (25), whereas accumulating observations suggest that degradation-independent mechanisms are also crucial for MDM2 in controlling p53 activities (26). Regardless, it is clear that the molecular mechanisms by which p53 activity is controlled are complex and how such mechanisms function in opposition to the Akt-signaling network remain to be elucidated.

Monocytic leukemia zinc finger (MOZ) protein is a MYST [MOZ, Ybf2/Something about silencing protein 3 (Sas3), Something about silencing protein 2 (Sas2), Tip60/KAT5]-type histone acetyltransferase (HAT) that functions as a coactivator for AML1- and p53-dependent transcription (27–29). $MOZ^{-/-}$ mice die at around embryonic day 15 (30). In serially passaged $MOZ^{-/-}$ MEFs, DNA damage-induced expression of p21 and ensuing cell-cycle arrest is profoundly impaired, suggesting that the p53 pathway may be altered in $MOZ^{-/-}$ MEFs (27). MOZ is involved in leukemia-associated chromosome rearrangements such as *t*(8, 16) (p11;p13) (31), *t*(8, 22) (32), and inv(8) (33), which result in fusion to the transcription coactivators CBP, p300, and transcriptional intermediary factor 2 (TIF2), respectively. Recently, we reported that MOZ directly interacts with p53 through its modification and selective activation of p21 but not Bcl-2 associated x protein (Bax) (27). Although MOZ stimulates p53-mediated transcription of the p21 gene selectively to induce cell-cycle arrest, neither the precise mechanisms of p53 transcriptional activation by MOZ nor the interactions between MOZ and p53 are fully understood.

In this report, we demonstrate that MOZ interacts with PML and recruits it into PML-NBs. A ternary p53–PML–MOZ interaction promotes the acetylation of p53 at K120 and K382 and subsequent p53-induced transcription of the p21 gene. Moreover, the MOZ amino acid sequence contains an Akt substrate motif, and phosphorylation of MOZ by Akt at T369 has a negative effect on its complex formation with PML. PML–MOZ complex formation, which is increased through PML-mediated Akt kinase activity suppression, induces acetylation of p53 and, consequently, p21 expression and p53-dependent premature senescence. These findings reveal a second mechanism that is distinct from Akt phosphorylation and activation of Mdm2, by which the Akt pathway counteracts p53 and prevents it from activating its downstream target genes.

Author contributions: S.R. and C.P. designed research; S.R. and S.M.A. performed research; O.L., Y.T., and I.K. contributed new reagents/analytic tools; S.R. and C.P. analyzed data; and S.R. and C.P. wrote the paper.

The authors declare no conflict of interest.

[1]To whom correspondence should be addressed. E-mail: clp3@columbia.edu.

This article contains supporting information online at www.pnas.org/lookup/suppl/doi:10.1073/pnas.1300490110/-/DCSupplemental.

Results

MOZ Interacts with PML in PML-NBs. PML is critical for the proper activation of p53 transcriptional activity (15, 16). Upon exposure to DNA damage (e.g., Ras activation, UV radiation), p53 becomes associated with PML-NBs. To investigate whether MOZ colocalizes with PML in PML-NBs, we exposed MCF-7 (breast cancer cell line) cells to UV radiation. In untreated cells, MOZ exhibited both speckled and diffuse nuclear staining in both the nucleoplasm and the nucleolus. When cells were exposed to UV radiation, both PML and MOZ showed a high degree of colocalization in PML-NBs (Fig. 1*A* and Fig. S1*A*). Coimmunoprecipitation analysis confirmed that both PML–MOZ and p53–MOZ interactions were increased after UV radiation, but not after treatment with As_2O_3 (Fig. 1*B* and Fig. S1 *B* and *C*). These results suggest that UV radiation enhances p53–PML–MOZ ternary complex formation.

To identify the PML-interacting domain in MOZ, the interactions between various deletion mutants of MOZ and PML were examined by immunoprecipitation (IP) immunoblotting. Coimmunoprecipitation experiments using these deletion mutants identified two PML-interacting regions (amino acids spanning 144–664 and 1517–1741) in MOZ (Fig. 1 *C* and *D* and Fig. S2*A*). To determine the region of PML required for binding to MOZ, a pulldown assay using anti-FLAG epitope peptide antibody (see *SI Materials and Methods*) was performed using a series of PML deletion mutants. Results from these studies suggest that PML possesses one MOZ-interacting coiled-coil domain within amino acids 229–360 (Fig. 1*E* and Fig. S2*B*).

To confirm that the interaction between PML and MOZ is direct, we performed a Far-Western blot analysis. In brief, full-length PML protein was translated in reticulocyte lysates, and then proteins were separated by SDS/PAGE, followed by transfer to nitrocellulose. Following denaturation and renaturation, proteins on the membrane were incubated with sf9 insect cells-purified MOZ proteins, and bound MOZ was detected by immunoblotting analysis. As shown in Fig. 1*F*, PML directly bound to MOZ in vitro. As negative controls, BSA and the polypeptides present in reticulocyte extracts did not interact with MOZ. Therefore, we conclude that PML is a bona fide interacting partner for MOZ.

PML-MOZ Association Enhances MOZ-Mediated p53 Acetylation and p21 Expression. PML directly interacts with HATs, including CBP, p300, and Tip60, and PML-NBs serve as sites for posttranslational modifications of p53 (17, 34). MOZ is a MYST-type HAT, like Tip60 and MOF (35, 36), and the MYST domain of MOZ has 69% homology with that of Tip60. We therefore hypothesized that MOZ may play an important role in acetylation of p53.

In fact, an in vitro acetylation assay showed that MOZ could acetylate p53 at K120 and K382 (Fig. 2*A* and Fig. S3). Furthermore, knockdown of MOZ expression partially inhibited irradiation-dependent acetylation of p53 at K120 and K382, but not at K373 (Fig. 2*B*). Therefore, MOZ displays aspects of both Tip60 and p300 in acetylation of p53. To further confirm that MOZ acetylates p53 at K120 and K382, we generated an acetylase-deficient MOZ variant (AD-MOZ: Q654E/G657E), in which the acetyl-CoA–binding sequences are mutated to glutamine, mimicking the MYST domain of a previously characterized acetylase-deficient mutant of Tip60 (37) (Fig. 2*C*). Immunoblotting showed that wild-type (WT) MOZ, but not AD-MOZ, could acetylate itself and p53 at K382 (Fig. S4 *A* and *B*). Because we observed that MOZ is recruited into PML-NBs like CBP/p300, we wanted to determine whether the PML–MOZ interaction could also be enhanced by MOZ-mediated acetylation of p53. To this end, we performed immunoblotting with antibodies that specifically recognize acetylated-p53 at K120 and K382 and showed that PML promotes MOZ-mediated p53 acetylation (Fig. 2*D*).

To test whether PML also affects transcriptional activation of the p53–MOZ complex, we used reporter plasmids under the control of promoters for p53 target genes such as p21 and bax in $MOZ^{-/-}$ MEFs. Whereas PML stimulated p53-mediated activation of p21-luc in wild-type MEFs, p21-luc induction was

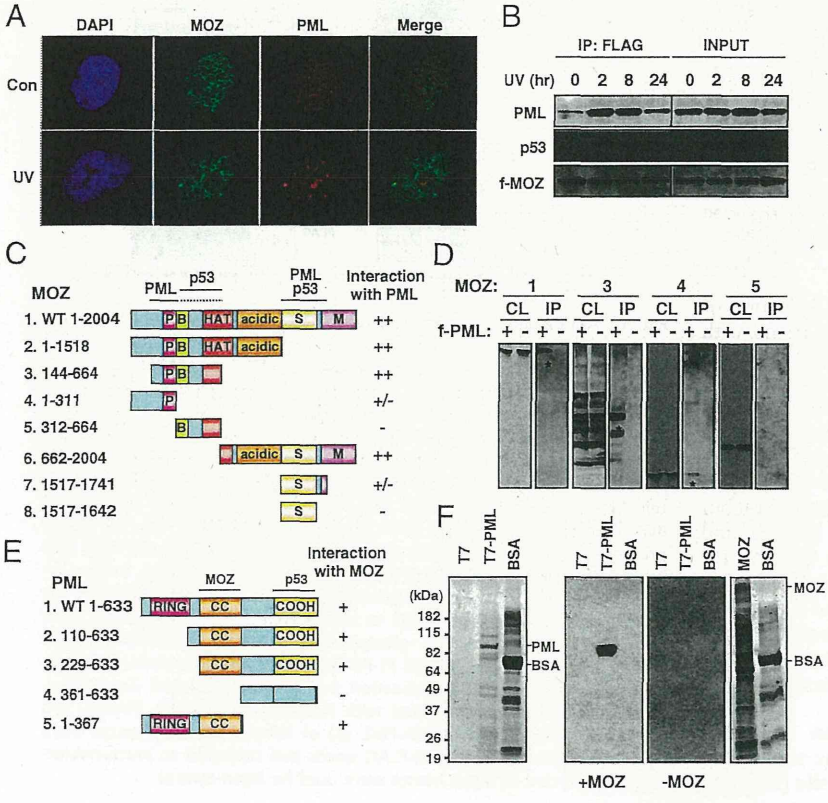

Fig. 1. MOZ is recruited into promyelocytic leukemia nuclear bodies after DNA damage. (*A*) Colocalization of MOZ with PML. MCF-7 cells were irradiated with UV (30 J/m^2) and then processed for immunofluorescence. (*B*) MOZ interacts with PML and p53. MCF7 cells were cotransfected with HA-epitope tagged PML and FLAG-epitope tagged MOZ and then subjected to UV irradiation (30 J/m^2) followed by harvesting at indicated times. The cell lysates were immunoprecipitated with anti-FLAG beads and subjected to immunoblotting. (*C*) Schematic representation of the structure of MOZ deletion mutants. The plant homeo domain (PHD) finger domain (P), the basic domain (B), the HAT domain, the serine-rich region (S), the methionine-rich region (M), and the regions required for interaction with PML (bars) and for strong interaction with PML (dotted bar) are indicated. (*D*) BOSC23 cells were transfected with HA-MOZ deletion mutants along with FLAG-PML. Cell lysates (CL) were immunoprecipitated with anti-FLAG beads and were subjected to immunoblotting. (*E*) Schematic representation of the structure of PML deletion mutants. The region required for interaction with MOZ is indicated (bar). (*F*) PML can interact with MOZ in vitro as indicated by Far-Western analysis. FLAG-MOZ protein purified from sf9 (*Right*) and HAPML immunoprecipitated from reticulocyte lysate (*Left*) were subjected to SDS/PAGE and stained by Coomassie blue. Mock (T7) and PML (T7-PML) proteins were resolved and transferred to a nitrocellulose membrane, which was then incubated with 1 μg/mL of purified FLAG-MOZ (*Center*) and detected by immunoblotting.

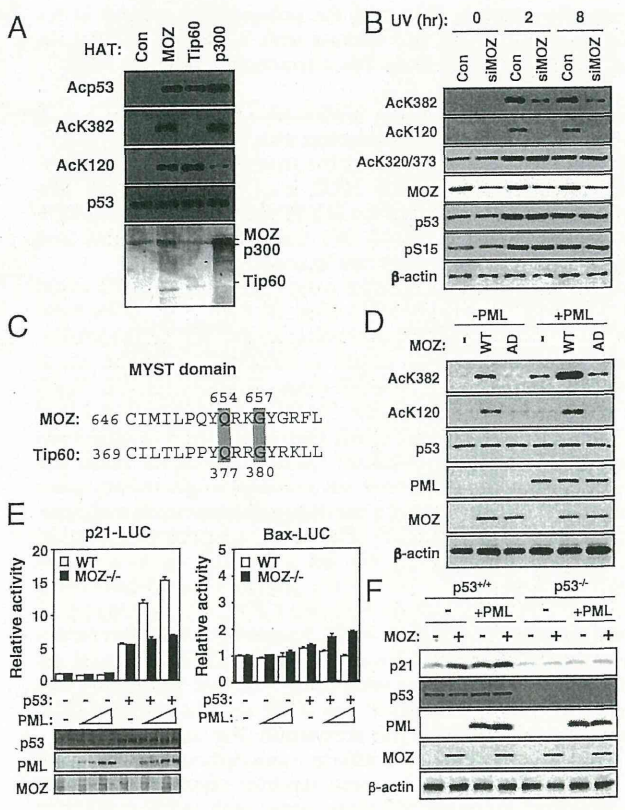

Fig. 2. MOZ acetylates p53 at K382 and K120. (*A*) In vitro acetylation of p53 by MOZ, Tip60, and p300. Baculovirus-expressed p53, MOZ, Tip60, and p300 were assayed for acetylation activity of p53. The acetylation samples were detected by immunoblotting with antibodies against Acp53, AcK382, AcK120, and p53 (*Upper*). MOZ, Tip60, and p300 proteins were visualized by silver staining (*Lower*). (*B*) Inhibition of MOZ blocks p53 acetylation. The siRNA-treated MCF-7 cells were irradiated with 30 J/m^2 of UV for indicated times and were subjected to immunoblotting. (*C*) MYST domain sequences of MOZ and Tip60. (*D*) PML enhances MOZ acetylation of p53. BOSC23 cells were transfected with indicated FLAG-p53 along with either HA-MOZ or PML and were subjected to immunoblotting. (*E*) PML enhances MOZ-mediated p21-luc but not Bax-luc reporter activity. Either wild-type (WT) or MOZ$^{-/-}$ MEFs were transfected with p21-luc (*Left*) or Bax-luc (*Right*), p53, PML, and pRL-CMV as a transfection control. (*F*) PML enhances MOZ-mediated p21 expression in a p53-dependent manner. Either HCT116 p53$^{+/+}$ or p53$^{-/-}$ cells were cotransfected with FLAG-MOZ along with HA-PML and were subjected to immunoblotting.

suppressed in MOZ$^{-/-}$ MEFs. On the other hand, induction of bax-luc was slightly induced in MOZ$^{-/-}$ MEFs compared with wild-type MEFs (Fig. 2*E*). This supports the likelihood that MOZ is a key component of the regulation of p53 by PML.

Although further luciferase and immunoblotting demonstrated that wild-type MOZ strongly enhanced *p21* gene transcription and *p21* expression in the presence of PML, AD-MOZ partially suppressed the expression of *p21* compared with wild-type MOZ, suggesting that MOZ-mediated acetylation of p53 is important but not sufficient for MOZ-mediated expression of p21 (Fig. 2*F* and Fig. S5). A MOZ-CBP fusion gene, produced by the *t*(8, 16) translocation, is associated with acute monocytic leukemia. We tested the effects of the MOZ-CBP chimera and found that MOZ-CBP suppressed p53-dependent transcriptional activation of p21 (Fig. S5). These results indicate that MOZ associates with PML and that the PML–MOZ complex induces p21 expression.

Akt Phosphorylates MOZ and Inhibits Its Interaction with PML. Analysis of the human MOZ sequence revealed one site (T369) that conforms to the Akt phosphorylation consensus site (Fig. 3*A*). The Akt phosphorylation motif (R-X-R-X-X-S/T-B, where "X" represents any amino acid and "B" represents a hydrophobic residue), has been refined to include amino acids that contribute to its 3D structure (38). We found that the Akt phosphorylation motif is also conserved in human-, mouse-, rat-MOZ, and RXRXXT in human MORF/MYST4, suggesting its possible functional importance. The presence of putative Akt phosphorylation sites in MOZ led us to determine whether MOZ is a substrate for Akt.

In fact, we observed that recombinant Akt was sufficient for inducing phosphorylation of wild-type MOZ in vitro, but not T369A-MOZ (Fig. 3*B*). We also confirmed that wild-type Akt, but not dominant negative (DN) Akt, was capable of inducing MOZ phosphorylation in vitro (Fig. 3*C*). To further examine whether Akt can phosphorylate MOZ at T369, we generated a polyclonal antibody that specifically recognizes MOZ phosphorylated at that site (pT369-MOZ). By immunoblotting, this antibody detected MOZ that had been phosphorylated at T369 by myristoylated active Akt (Myr) while it partially cross-reacted with nonphosphorylated MOZ in a manner similar to a pAkt-substrate antibody that recognized phosphorylated MOZ (Fig. 3*D*). These results support the possibility that Akt mediates MOZ phosphorylation at T369 in vivo and in vitro.

Because T369 of MOZ is located within the PML-binding domain, we further tested whether this phosphorylation affects binding between MOZ and PML or p53 (Fig. 1*C*). Coimmunoprecipitation

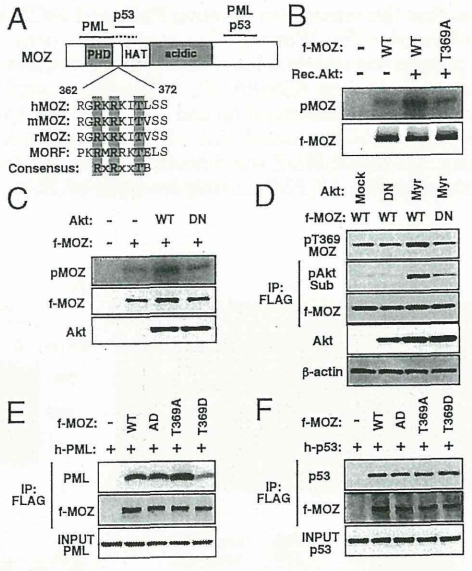

Fig. 3. Akt-mediated phosphorylation of MOZ suppresses the interaction between PML and MOZ. (*A*) Structure of the consensus Akt phosphorylation motif in MOZ. Sequences of human-, mouse-, rat-MOZ, and MORF are shown for comparison. (*B*) Recombinant Akt phosphorylates MOZ in vitro. FLAG-tagged wild-type (WT) and T369A (TA) of MOZ proteins were immunoprecipitated with anti-FLAG beads from transfected BOSC23 cells. MOZ proteins were incubated with recombinant Akt (Rec. Akt) in the presence of [γ-^{32}P] ATP. (*C*) FLAG-tagged WT and dominant negative (DN) Akt and MOZ proteins were immunoprecipitated with anti-FLAG beads from transfected BOSC23 cells. MOZ proteins were incubated with WT- or DN-Akt in the presence of [γ-^{32}P]ATP. (*D*) Akt phosphorylates MOZ at T369. BOSC23 cells were cotransfected with FLAG-tagged WT- or TA-MOZ along with myristoylated (Myr)- or DN-Akt. Cell lysates were immunoprecipitated with anti-FLAG beads and were subjected to immunoblotting using antibodies for phospho-T369 (pT369-MOZ), phospho-Akt substrate (pAkt-Sub), FLAG (MOZ), Akt, and β-actin. (*E* and *F*) Akt-mediated phosphorylation of MOZ suppresses the PML–MOZ interaction but not the p53–MOZ interaction. BOSC23 cells were cotransfected with FLAG-tagged WT, AD, T369A, and T369D of MOZ along with HA-PML (*E*) or HA-p53 (*F*). Cell lysates were immunoprecipitated with anti-FLAG beads and subjected to immunoblotting. Ten percent of input lysates were used for input control.

analysis using phosphorylation-deficient MOZ (T369A) demonstrated that it had increased interaction with PML (Fig. 3*E*). Interestingly, these mutations did not affect MOZ-p53 binding (Fig. 3*F*). These results indicate that Akt phosphorylates T369 of MOZ to inhibit its interaction with PML.

Phosphorylation of MOZ at T369 Is Important for Negative Regulation of p53 Acetylation. Because the interaction between PML and MOZ is likely dependent on the phosphorylation state of MOZ at T369, we determined whether Akt-mediated phosphorylation of MOZ inhibits its acetylation activity. An IP immunoblotting showed that T369A-MOZ strongly acetylates p53 at K382 and K120 in transfected cells, unlike the phosphorylation-mimicking mutant T369D-MOZ (Fig. 4*A*). To examine the T368A-MOZ acetylation activity per se, we next performed an in vitro HAT activity assay using histone peptides as substrates. In contrast to Fig. 4*A*, T369A-MOZ showed only slightly increased acetylation of histone H3 and H4 peptides compared with T369D-MOZ (Fig. 4*B*). These results are consistent with results showing that wild-type or T369 mutant forms of MOZ displayed equivalent abilities to self-acetylate and that the acetylation activity of MOZ was enhanced in the presence of PML (Fig. 4*C*). Thus, our data indicate that phosphorylation of MOZ at T369 is important for the negative regulation of acetylation of p53 in the presence of PML, whereas such phosphorylation is not important for its acetylation activity per se.

Further luciferase analysis and real-time PCR analysis upon coexpression of MOZ with PML revealed that T369A-MOZ strongly enhanced the expression of p21, whereas T369D-MOZ partially suppressed the expression of p21 compared with T369A-MOZ (Fig. 4 *D* and *E*). These data are consistent with p21 expression analyzed by immunoblotting (Fig. 4*F*). Taken together, these findings indicate that suppression of Akt-mediated phosphorylation at T369 of MOZ is critical for MOZ recruitment into PML-NBs and its acetylation of p53. We conclude that the PI3K-Akt pathway-mediated suppression of p21 is not only through Akt phosphorylation and stabilization of MDM2, but also through blocking the recruitment of MOZ into PML-NBs and the acetylation of p53.

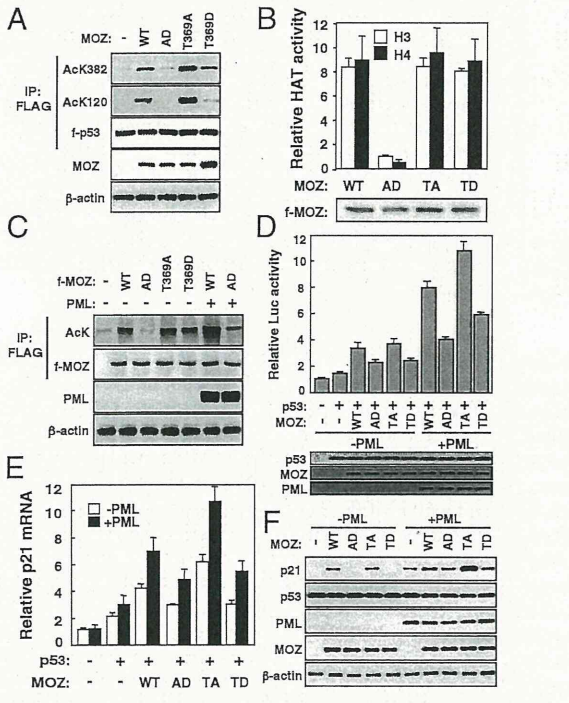

Fig. 4. Phosphorylation of MOZ is important for negative regulation of p53 acetylation. (*A*) BOSC23 cells were cotransfected with HA-tagged WT, AD, T369A or T369D along with FLAG-p53. Cell lysates were purified with anti-FLAG beads and were subjected to immunoblotting using antibodies for AcK382, AcK120, FLAG (f-p53), HA (MOZ), and β-actin. (*B*) Phosphorylation of MOZ has no effect on HAT activity. FLAG-tagged WT, AD, T369A, and T369D MOZ were purified with anti-FLAG beads from transfected BOSC23 cells. The acetylase activities of mutant MOZ were measured as described in *Materials and Methods*. (*C*) BOSC23 cells were cotransfected with FLAG-tagged WT, AD, T369A, or T369D of MOZ with HA-PML. Cell lysates were immunoprecipitated with anti-FLAG beads and subjected to immunoblotting. (*D*) The PML–MOZ interaction stimulates p53-mediated p21 reporter activity. H1299 cells were cotransfected with p21-luc, p53, and PML along with WT, AD, T369A, or T369D of MOZ. (*E* and *F*) The PML–MOZ interaction stimulates p53-dependent p21 induction and expression. H1299 cells were cotransfected with p53 and PML along with HA-tagged WT, AD, T369A, and T369D of MOZ. The harvested cells were subjected to real-time PCR (*E*) and to immunoblotting.

Loss of MOZ Contributes to Resistance to PML-Induced Senescence. To characterize PML expression-induced cell-cycle arrest and senescence, we infected wild-type and MOZ$^{-/-}$ primary mouse embryonic fibroblasts (pMEFs) with a pLNCX retroviral vector expressing PML and Ha-Ras Ha-Ras (v-Ha-ras Harvey rat sarcoma viral oncogene homolog, V12), cultured them for 3 d under puromycin selection, and counted cells for the next 5 d. Wild-type pMEFs expressing PML as well as oncogenic Ha-Ras (V12) ceased to proliferate at subconfluent densities (Fig. 5*A*). Conversely, in MOZ$^{-/-}$ pMEFs, ectopic PML expression did not lead to cessation of proliferation, although RasV12-expressing MOZ$^{-/-}$ MEFs exhibited slowed proliferation (Fig. 5*B*). The morphology of MOZ$^{-/-}$ pMEFs differed from senescent wild-type pMEFs, even after infection of these cells with retroviruses containing PML or Ras (**Fig. S6**).

We next examined the cell-cycle distribution of pMEFs arrested by retroviral-mediated PML expression by following BrdU incorporation. Wild-type pMEFs did not incorporate BrdU (Fig. 5 *C* and *D*) and became positive for senescence-associated β-galactosidase (SA β-gal) staining, a marker of cellular senescence (Fig. 5*E* and **Fig. S7**). Consistent with Fig. 5*B*, forced PML expression in MOZ$^{-/-}$ pMEFs did not alter BrdU incorporation (Fig. 5 *C* and *D*). The frequency of SA β-gal–positive cells was markedly lower in PML-expressing MOZ$^{-/-}$ pMEF cells than in wild-type pMEFs (Fig. 5*E* and **Fig. S7**). These results indicate that loss of MOZ contributes to resistance to PML-induced premature senescence.

Based on the above findings, we examined p53 modifications and p21 expression in WT and MOZ$^{-/-}$ MEFs expressing either RasV12 or PML. Although both p53 and p16 are vital components of the intracellular senescence pathway (39), PML does not affect p16 expression (17), consistent with our observed results (Fig. 5*F*). Although ectopically expressed Ras or PML induced equivalent levels of p53 in both wild-type and MOZ$^{-/-}$ MEFs, their expression led to the appearance of more nonphosphorylated MOZ in wild-type cells, which corresponded to increased acetylation of p53 at K117 and K379 (equivalent to human p53 K120 and K382, respectively). In line with this, p21 expression was induced in wild-type pMEFs, but not in MOZ$^{-/-}$ pMEFs after PML expression despite similar p53 transcriptional levels in wild-type and MOZ$^{-/-}$ pMEFs (Fig. 5*F* and **Fig. S8**). This suggests that, through PML-mediated suppression of the Akt pathway, increased PML–MOZ complex formation enhances p21 expression, which mediates p53-dependent premature senescence upon PML overexpression. In short, MOZ is crucial for p53-mediated p21 expression induced by PML expression and the ensuing PML-induced senescence.

Discussion

Several factors, such as Tip60, hematopoietic zinc finger (Hzf), and human cellular apoptosis susceptibility protein (hCAS/CSE1L) are involved in the selection of p53 target genes (35, 40, 41). However, the molecular mechanisms by which p53 "chooses" cell-cycle arrest or apoptosis are not fully understood. Here we discovered that the MYST-type HAT MOZ interacts with PML and is recruited into PML-NBs. Significantly, we confirmed that the

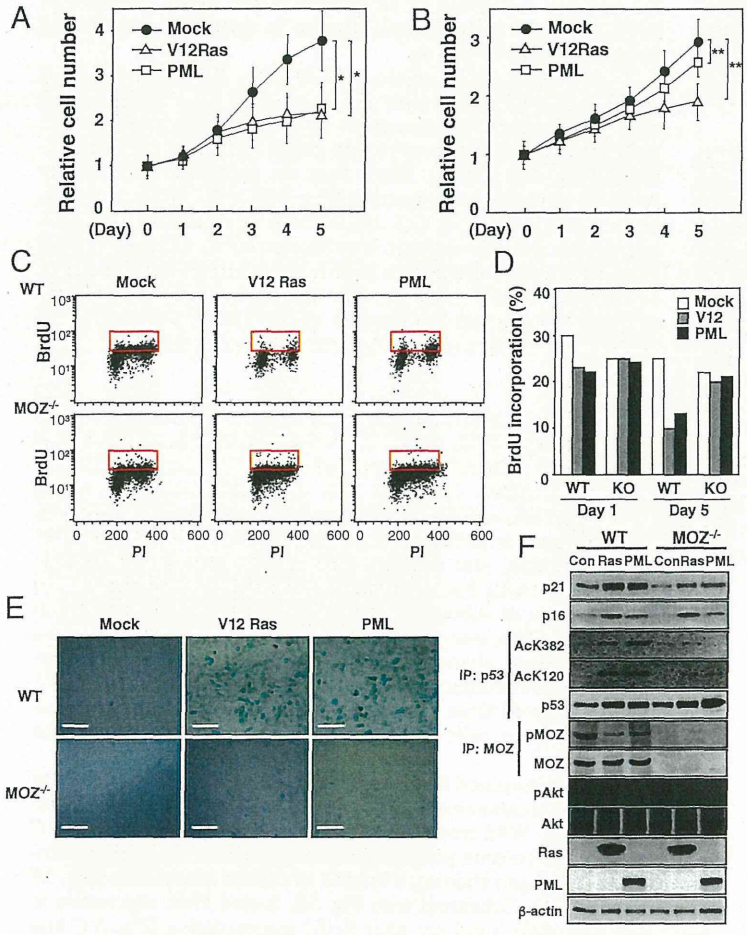

Fig. 5. MOZ-knockout cells display resistance to PML-induced senescence. (*A* and *B*) Growth curves of wild-type (*A*) and MOZ$^{-/-}$ (*B*) pMEFs infected with vector (Mock), RasV12, or PML. Day 0 is the first day after puromycin selection. Error bars represent the standard deviation for three independent littermate experiments. *$P < 0.02$, **$P > 0.03$. (*C*) Flow cytometry analysis of pMEFs. pMEFs in growth phase were stained with an anti-BrdU antibody and propidium iodide at 5 d after selection. (*D*) Histogram comparing BrdU incorporation of RasV12- and PML-infected pMEFs at 1 or 5 d after selection. (*E*) SA β-gal staining of WT or MOZ$^{-/-}$ pMEFs infected with pLNCX (Mock), RasV12, or PML at 5 d after selection. (Scale bars: 50 μm.) (*F*) MOZ$^{-/-}$ cells are resistant to PML-induced p21 expression. The infected WT or MOZ$^{-/-}$ pMEFs were harvested at 5 d after selection. The cells were partially subjected to immunoprecipitation with anti-p53 (IP: p53) and anti-MOZ (IP: MOZ) and were subjected to immunoblotting using indicated antibodies.

PML–MOZ interaction promotes the MOZ-mediated acetylation of p53 at K120 and K382, which makes MOZ distinct from other KATs that can target only one of these residues and p53-mediated expression of p21 (Fig. S9).

It has been reported that p53 can be acetylated at K373, K382, K164 (catalyzed by p300/CBP), K320 (PCAF/KAT2B), and K120 (Tip60) (42, 43). Although p53 mice engineered to lack acetylatable lysines within their C termini are viable and phenotypically normal, p53-mediated transcriptional activation upon DNA damage is partially impaired in the ES cells and thymocytes of these mice (44). In addition, the p53 7KR mutation, where the seven C-terminal lysines were changed to arginine, significantly contributes to hematopoietic stem cell homeostasis and mouse radiosensitivity (45). Thus, it is possible that other cofactors or additional acetylation sites of p53 may compensate for the loss of p53 acetylation at the C terminus. In this report, we found that MOZ is an acetylation regulator of p53. In contrast to normal MOZ and CBP, the leukemia-associated MOZ-CBP fusion protein inhibited p53-mediated transcription (Fig. S5). These results suggest that inhibition of MOZ-p53–mediated transcription might be involved in pathogenesis of tumors and leukemia.

Our previous study revealed that MOZ-deficient MEFs exhibit impaired p21 expression and fail to arrest in G1 phase in response to DNA damage (27). Evidence of the significance of lysine modifications in the functions of the DNA-binding region comes from studies showing that Tip60/KAT5 and hMOF/KAT8, members of the MYST family of acetyltransferases, acetylate K120 of p53 followed by its accumulation on Puma and Bax promoters (35) and that K120/K164R double-mutant mice display reduced induction of *p21* and *puma* (43). In addition, K120 acetylation of p53 exhibited specific DNA binding and discriminated among response elements at effective physiological salt concentration (46). The ability of MOZ to simultaneously acetylate both K120 and K382 might be responsible for the difference of target genes from previous reports. It might be also possible that MOZ acetylation of p53 occurs in a different subcellular compartment, such as PML-NBs, from that of Tip60/hMOF. Thus, the DNA-binding domain acetylation by MOZ appears to play a role in selective gene regulation.

Akt kinase activity is frequently elevated in several high-grade, late-stage cancers (47), and a somatic constitutively active Akt mutant has been identified in human breast, colorectal, and ovarian cancers (48). In fact, the role of Akt in the p53-mediated response was shown to involve Akt suppression of p21 expression through phosphorylation and activation of MDM2 and subsequent MDM2-mediated ubiquitination of p53 (23, 24, 49). Here we demonstrate that Akt works by a second process in which Akt phosphorylation of MOZ at T369 within its PML interaction region blocks its complex formation with PML (Fig. 3*A*). A mutant MOZ (T369A) displays enhanced acetylation of p53 at K120 and K382 with ensuing increased expression of p21, indicating that phosphorylation at T369 of MOZ is important for the acetylation of p53, but not for its acetylation activity per se (Fig. 4*A* and *C*). Suppressing Akt-mediated phosphorylation of MOZ at T369 is likely very important for the recruitment of MOZ into PML-NBs and the subsequent acetylation of p53.

In this report, we demonstrate that forced PML expression in MOZ$^{-/-}$ primary MEFs somewhat suppresses either G1 arrest or senescence (Fig. 5*B*). PML expression in MOZ$^{-/-}$ MEFs only slightly alters BrdU incorporation (Fig. 5 *C* and *D*), but the frequency of SA β-gal–positive senescent cells is markedly lower (Fig. 5*E* and Fig. S7). These results indicate that loss of MOZ contrib-

utes to resistance to PML-induced G1 arrest and premature senescence. In contrast, MOZ$^{-/-}$ primary MEFs exhibit a high proportion of cells in S phase but lower BrdU incorporation after forced PML expression. This is also true for serially passaged MEFs after DNA damage, suggesting that MOZ might be involved in DNA replication. These results are consistent with a report that depletion of inhibitor of growth family, member 5 (ING5), which comprises a subunit of the ING5-MOZ stoichiometric HAT complex, renders cells unable to complete S phase, allowing only a few cells to proceed to the G2/M phase. Together, these results suggest that ING5–MOZ complexes are essential for DNA replication, not only for initiation but also for replication fork movement (50). Recently, it has been reported that Pten-loss–induced cellular senescence, where the activation of the PI3K-Akt pathway is the key mechanism triggering a p53-dependent senescence, represents a senescence response that is distinct from oncogene-induced senescence (51). Further studies are required to investigate whether the sequential phenomenon—down-regulation of Akt activity and MOZ acetylation of p53—occurs in the PML-NB subcellular compartment.

Materials and Methods

Plasmids expressing FLAG-tagged and HA-tagged human MOZ, CBP, MOZ-CBP, and p300 were cloned into the pLNCX vector (Clontech). Human cDNA encoding FLAG- and HA-tagged PML isoform IV and HA-tagged V12 Ras were cloned into pLPCX retrovirus vectors. Myristoylated active, FLAG-tagged, wild-type, or dominant negative Akt1 were described previously (52). Details of other methods used in this article, including cell culture, antisense oligonucleotides, baculovirus protein expression and purification, flow cytometry, SA β-gal assay, immunofluorescence, immunoprecipitation, immunoblotting, Far-Western blotting, real-time PCR, luciferase assay, in vitro acetylation assay, and in vitro kinase assay are described in ***SI Materials and Methods***.

ACKNOWLEDGMENTS. Baculovirus expressing His_6-tagged p300 was a generous gift from Dr. W. L. Kraus. We thank Ella Freulich for expert technical assistance. This work was supported in part by Grants-in-Aid for Scientific Research from the Ministry of Health, Labor, and Welfare; the Ministry of Education, Culture, Sports, Science, and Technology (to I.K. and S.R.); The Mochida Memorial Foundation for Medical and Pharmaceutical Research (to S.R.); and by National Institutes of Health Grant CA77742 (to C.P.).

1. Vogelstein B, Lane D, Levine AJ (2000) Surfing the p53 network. *Nature* 408(6810): 307–310.
2. Vousden KH, Lu X (2002) Live or let die: The cell's response to p53. *Nat Rev Cancer* 2(8):594–604.
3. Laptenko O, Prives C (2006) Transcriptional regulation by p53: One protein, many possibilities. *Cell Death Differ* 13(6):951–961.
4. Harris SL, Levine AJ (2005) The p53 pathway: Positive and negative feedback loops. *Oncogene* 24(17):2899–2908.
5. Vousden KH, Prives C (2009) Blinded by the light: The growing complexity of p53. *Cell* 137(3):413–431.
6. Alcalay M, et al. (1998) The promyelocytic leukemia gene product (PML) forms stable complexes with the retinoblastoma protein. *Mol Cell Biol* 18(2):1084–1093.
7. Vallian S, et al. (1998) Modulation of Fos-mediated AP-1 transcription by the promyelocytic leukemia protein. *Oncogene* 16(22):2843–2853.
8. Zhang Y, Xiong Y (1999) Mutations in human ARF exon 2 disrupt its nucleolar localization and impair its ability to block nuclear export of MDM2 and p53. *Mol Cell* 3(5):579–591.
9. de Thé H, et al. (1991) The PML-RAR alpha fusion mRNA generated by the t(15;17) translocation in acute promyelocytic leukemia encodes a functionally altered RAR. *Cell* 66(4):675–684.
10. Pandolfi PP, et al. (1991) Structure and origin of the acute promyelocytic leukemia myl/RAR alpha cDNA and characterization of its retinoid-binding and transactivation properties. *Oncogene* 6(7):1285–1292.
11. Piazza F, Gurrieri C, Pandolfi PP (2001) The theory of APL. *Oncogene* 20(49):7216–7222.
12. LaMorte VJ, Dyck JA, Ochs RL, Evans RM (1998) Localization of nascent RNA and CREB binding protein with the PML-containing nuclear body. *Proc Natl Acad Sci USA* 95(9): 4991–4996.
13. Zhong S, et al. (2000) Role of SUMO-1-modified PML in nuclear body formation. *Blood* 95(9):2748–2752.
14. Ferbeyre G, et al. (2000) PML is induced by oncogenic ras and promotes premature senescence. *Genes Dev* 14(16):2015–2027.
15. Fogal V, et al. (2000) Regulation of p53 activity in nuclear bodies by a specific PML isoform. *EMBO J* 19(22):6185–6195.
16. Guo A, et al. (2000) The function of PML in p53-dependent apoptosis. *Nat Cell Biol* 2(10):730–736.
17. Pearson M, et al. (2000) PML regulates p53 acetylation and premature senescence induced by oncogenic Ras. *Nature* 406(6792):207–210.
18. Barlev NA, et al. (2001) Acetylation of p53 activates transcription through recruitment of coactivators/histone acetyltransferases. *Mol Cell* 8(6):1243–1254.
19. Ito A, et al. (2001) p300/CBP-mediated p53 acetylation is commonly induced by p53-activating agents and inhibited by MDM2. *EMBO J* 20(6):1331–1340.
20. Yao TP, et al. (1998) Gene dosage-dependent embryonic development and proliferation defects in mice lacking the transcriptional integrator p300. *Cell* 93(3):361–372.
21. Trotman LC, et al. (2006) Identification of a tumour suppressor network opposing nuclear Akt function. *Nature* 441(7092):523–527.
22. Sabbatini P, McCormick F (1999) Phosphoinositide 3-OH kinase (PI3K) and PKB/Akt delay the onset of p53-mediated, transcriptionally dependent apoptosis. *J Biol Chem* 274(34):24263–24269.
23. Mayo LD, Donner DB (2001) A phosphatidylinositol 3-kinase/Akt pathway promotes translocation of Mdm2 from the cytoplasm to the nucleus. *Proc Natl Acad Sci USA* 98(20):11598–11603.
24. Zhou BP, et al. (2001) HER-2/neu induces p53 ubiquitination via Akt-mediated MDM2 phosphorylation. *Nat Cell Biol* 3(11):973–982.
25. Minsky N, Oren M (2004) The RING domain of Mdm2 mediates histone ubiquitylation and transcriptional repression. *Mol Cell* 16(4):631–639.
26. Pant V, Xiong S, Iwakuma T, Quintás-Cardama A, Lozano G (2011) Heterodimerization of Mdm2 and Mdm4 is critical for regulating p53 activity during embryogenesis but dispensable for p53 and Mdm2 stability. *Proc Natl Acad Sci USA* 108(29):11995–12000.
27. Rokudai S, et al. (2009) Monocytic leukemia zinc finger (MOZ) interacts with p53 to induce p21 expression and cell-cycle arrest. *J Biol Chem* 284(1):237–244.
28. Champagne N, Pelletier N, Yang XJ (2001) The monocytic leukemia zinc finger protein MOZ is a histone acetyltransferase. *Oncogene* 20(3):404–409.
29. Kitabayashi I, Aikawa Y, Nguyen LA, Yokoyama A, Ohki M (2001) Activation of AML1-mediated transcription by MOZ and inhibition by the MOZ-CBP fusion protein. *EMBO J* 20(24):7184–7196.
30. Katsumoto T, et al. (2006) MOZ is essential for maintenance of hematopoietic stem cells. *Genes Dev* 20(10):1321–1330.
31. Borrow J, et al. (1996) The translocation t(8;16)(p11;p13) of acute myeloid leukaemia fuses a putative acetyltransferase to the CREB-binding protein. *Nat Genet* 14(1):33–41.
32. Chaffanet M, et al. (2000) MOZ is fused to p300 in an acute monocytic leukemia with t(8;22). *Genes Chromosomes Cancer* 28(2):138–144.
33. Carapeti M, Aguiar RC, Goldman JM, Cross NC (1998) A novel fusion between MOZ and the nuclear receptor coactivator TIF2 in acute myeloid leukemia. *Blood* 91(9):3127–3133.
34. Wu Q, et al. (2009) PML3 orchestrates the nuclear dynamics and function of TIP60. *J Biol Chem* 284(13):8747–8759.
35. Sykes SM, et al. (2006) Acetylation of the p53 DNA-binding domain regulates apoptosis induction. *Mol Cell* 24(6):841–851.
36. Tang Y, Luo J, Zhang W, Gu W (2006) Tip60-dependent acetylation of p53 modulates the decision between cell-cycle arrest and apoptosis. *Mol Cell* 24(6):827–839.
37. Ikura T, et al. (2000) Involvement of the TIP60 histone acetylase complex in DNA repair and apoptosis. *Cell* 102(4):463–473.
38. Alessi DR, Caudwell FB, Andjelkovic M, Hemmings BA, Cohen P (1996) Molecular basis for the substrate specificity of protein kinase B: Comparison with MAPKAP kinase-1 and p70 S6 kinase. *FEBS Lett* 399(3):333–338.
39. Lin AW, et al. (1998) Premature senescence involving p53 and p16 is activated in response to constitutive MEK/MAPK mitogenic signaling. *Genes Dev* 12(19):3008–3019.
40. Das S, et al. (2007) Hzf determines cell survival upon genotoxic stress by modulating p53 transactivation. *Cell* 130(4):624–637.
41. Tanaka T, Ohkubo S, Tatsuno I, Prives C (2007) hCAS/CSE1L associates with chromatin and regulates expression of select p53 target genes. *Cell* 130(4):638–650.
42. Gu W, Roeder RG (1997) Activation of p53 sequence-specific DNA binding by acetylation of the p53 C-terminal domain. *Cell* 90(4):595–606.
43. Tang Y, Zhao WH, Chen Y, Zhao Y, Gu W (2008) Acetylation is indispensable for p53 activation. *Cell* 133(4):612–626.
44. Krummel KA, Lee CJ, Toledo F, Wahl GM (2005) The C-terminal lysines fine-tune P53 stress responses in a mouse model but are not required for stability control or transactivation. *Proc Natl Acad Sci USA* 102(29):10188–10193.
45. Wang YV, et al. (2011) Fine-tuning p53 activity through C-terminal modification significantly contributes to HSC homeostasis and mouse radiosensitivity. *Genes Dev* 25(13):1426–1438.
46. Arbely E, et al. (2011) Acetylation of lysine 120 of p53 endows DNA-binding specificity at effective physiological salt concentration. *Proc Natl Acad Sci USA* 108(20):8251–8256.
47. Sun M, et al. (2001) AKT1/PKBalpha kinase is frequently elevated in human cancers and its constitutive activation is required for oncogenic transformation in NIH3T3 cells. *Am J Pathol* 159(2):431–437.
48. Carpten JD, et al. (2007) A transforming mutation in the pleckstrin homology domain of AKT1 in cancer. *Nature* 448(7152):439–444.
49. Michael D, Oren M (2002) The p53 and Mdm2 families in cancer. *Curr Opin Genet Dev* 12(1):53–59.
50. Doyon Y, et al. (2006) ING tumor suppressor proteins are critical regulators of chromatin acetylation required for genome expression and perpetuation. *Mol Cell* 21(1):51–64.
51. Alimonti A, et al. (2010) A novel type of cellular senescence that can be enhanced in mouse models and human tumor xenografts to suppress prostate tumorigenesis. *J Clin Invest* 120(3):681–693.
52. Rokudai S, Fujita N, Kitahara O, Nakamura Y, Tsuruo T (2002) Involvement of FKHR-dependent TRADD expression in chemotherapeutic drug-induced apoptosis. *Mol Cell Biol* 22(24):8695–8708.

Ayako Haga[1,2]
Yoko Ogawara[3]
Daisuke Kubota[1]
Issay Kitabayashi[3]
Yasufumi Murakami[2]
Tadashi Kondo[1]

[1]Division of Pharmaco-proteomics, National Cancer Center Research Institute, Tsukiji, Chuo-ku, Tokyo, Japan
[2]Department of Biological Science and Technology, Faculty of Industrial Science and Technology, Tokyo University of Science, Yamazaki, Noda-shi, Chiba, Japan
[3]Division of Hematological Malignancy, National Cancer Center Research Institute, Tsukiji, Chuo-ku, Tokyo, Japan

Received December 3, 2012
Revised January 21, 2013
Accepted January 29, 2013

Research Article

Interactomic approach for evaluating nucleophosmin-binding proteins as biomarkers for Ewing's sarcoma

Nucleophosmin (NPM) is a novel prognostic biomarker for Ewing's sarcoma. To evaluate the prognostic utility of NPM, we conducted an interactomic approach to characterize the NPM protein complex in Ewing's sarcoma cells. A gene suppression assay revealed that NPM promoted cell proliferation and the invasive properties of Ewing's sarcoma cells. FLAG-tag-based affinity purification coupled with liquid chromatography-tandem mass spectrometry identified 106 proteins in the NPM protein complex. The functional classification suggested that the NPM complex participates in critical biological events, including ribosome biogenesis, regulation of transcription and translation, and protein folding, that are mediated by these proteins. In addition to JAK1, a candidate prognostic biomarker for Ewing's sarcoma, the NPM complex, includes 11 proteins known as prognostic biomarkers for other malignancies. Meta-analysis of gene expression profiles of 32 patients with Ewing's sarcoma revealed that 6 of 106 were significantly and independently associated with survival period. These observations suggest a functional role as well as prognostic value of these NPM complex proteins in Ewing's sarcoma. Further, our study suggests the potential applications of interactomics in conjunction with meta-analysis for biomarker discovery.

Keywords:
Biomarker / Ewing's sarcoma / Interactome / Nucleophosmin
DOI 10.1002/elps.201200661

Additional supporting information may be found in the online version of this article at the publisher's web-site

1 Introduction

Cancer is a genetically and clinically diverse disease, and patients often exhibit different responses to treatment even when they are diagnosed at the same clinical stage. Clinical staging and pathological grading systems were established to estimate the clinical outcome of patients, and these systems are widely used to select the proper therapeutic approach. Molecular biomarkers support these modalities [1]. The proteome represents the functional translation of the genome and directly regulates cancer phenotypes. Therefore, proteomics is a promising approach to identify candidate biomarker. We previously reported the use of proteomics approaches to identify tissue biomarker candidates that can predict metastasis and response to treatment by patients with various types of malignancies [2]. Besides their clinical utility, biomarkers may pave the way to better understand cancer biology, because biomarkers correlate significantly with clinically important events. In addition to validation studies for clinical applications, the molecular properties of candidate biomarkers should be considered for further understanding of disease mechanisms.

Ewing's sarcoma is the second most common primary bone malignancy in children and adolescents. Despite significant progress in the development of intensive chemotherapy protocols and local control measures, 30–40% of patients with localized Ewing's sarcoma and 80% of patients with metastatic Ewing's sarcoma at diagnosis die within 5 years because of disease progression [3]. Although adjuvant chemotherapy is effective for treating patients with Ewing's sarcoma, intensive chemotherapy often causes serious side effects [4]. Therefore, prognostic and predictive biomarkers have long been required to select the patients for

Correspondence: Dr. Tadashi Kondo, Division of Pharmacoproteomics, National Cancer Center Research Institute, 5-1-1 Tsukiji, Chuo-ku, Tokyo 104-0045, Japan
E-mail: takondo@ncc.go.jp
Fax: +81-3-3547-5298

Abbreviations: DFS, disease-free survival; **FCS**, fetal calf serum; **IEF**, isoelectric focusing; **NPM**, nucleophosmin; **OS**, overall survival; **ROC**, receiver operator characteristic

intensive adjuvant therapy and to avoid unnecessary risk of side effects.

We previously performed proteomic studies using surgical specimens from patients with Ewing's sarcoma with different prognoses [5]. We found that the prognosis was significantly poorer for Ewing's sarcoma patients with nucleophosmin (NPM)-positive primary tumors than for those with NPM-negative primary tumors [5]. NPM is a nuclear phosphoprotein and is involved in the biogenesis of ribosomes, transportation of small basic proteins to the nucleolus, and diverse cellular functions [6]. Upregulation, mutation, and chromosomal translocation of *NPM1* occur in various malignancies [7–13]. Although these lines of evidence suggest functional association of NPM with carcinogenesis and cancer progression, the role of NPM in Ewing's sarcoma was not investigated until our studies were performed [5].

Recent progress in mass spectrometry (MS) facilitates the identification with high sensitivity of the components of protein complexes as well as the investigation of protein interactions (interactome studies). MS serves as one of the major techniques for elucidating the molecular mechanisms underlying disease [14, 15]. Interactome studies of target proteins can reveal novel functional properties under normal and pathological conditions. MS analyses revealed that NPM interacts with various proteins [16], including MDM2 [17], P53 [18], c-MYC [19], and ARF [20] and regulates their activities. Although protein–protein interactions may be cell-type specific, there is no report, to our knowledge, describing an interactomic approach to the NPM protein complex in Ewing's sarcoma cells.

In this study, we performed an interactome study on the NPM protein complex in Ewing's sarcoma cells with the goal of revealing its molecular properties and potential to serve as a prognostic marker for patients with Ewing's sarcoma. FLAG-tag-based affinity purification coupled with LC-MS/MS was employed, and the clinical utilities of the identified proteins were assessed by analysis of the literature and meta-analysis. We demonstrated here the potential utility of the interactomic approach for biomarker research.

2 Materials and methods

2.1 Cell culture

The Ewing's sarcoma cell lines NCR-EW2 [21], W-ES cells [22], and RD-ES (American Type Culture Collection, HTB-166) were cultured in RPMI 1640 medium supplemented with 10% fetal calf serum (FCS). These cells were maintained in an incubator at 37°C in an atmosphere of 5% CO_2. PLAT-F cells [23] were cultured in DMEM supplemented with 10% FCS.

2.2 Plasmid construction and transfection

The N-terminal FLAG-tagged NPM was generated by PCR using the deoxyoligonucleotides 5′-gactagcggccg caccatggcagactacaaggacgacgatgacaaggaagattcgatgga-3′ and 5′-tcagtatcgatttaaagagacttcctccactgccag-3′ as sense and antisense primers, respectively. pCR-Blunt vector (Invitrogen, Carlsbad, CA, USA) was digested at 37°C for 2 h with *Stu*I (NEB, Beverly, MA, USA). The PCR products were inserted into digested pCR-Blunt vector using T4 ligase (NEB) at 16°C overnight. FLAG-tagged NPM fragments were digested using *Eco*RI (NEB) and ligated into pMYs-IG (Cell Biolabs, San Diego, CA, USA).

PLAT-F cells were seeded in 10-cm dishes and transfected with 10 μg DNA by using 20 μL of GeneJuice Transfection Reagent (Novagen, Darmstadt, Germany) per dish. The culture supernatants were collected 24 h after transfection. For viral infection, 1.0×10^5 of Ewing's sarcoma cells (NCR-EW2, RD-ES, and W-ES) were seeded in six-well plates and incubated in the culture supernatant of PLAT-F transfectants with 8 μg/mL of polybrene for 24 h. Enhanced Green Fluorescent Protein-positive cells were sorted with a fluorescence activated cell sorter (JSAN Cell Sorter, Bay Bioscience, Japan).

2.3 shRNA transfection

Two human lentiviral shRNA clones targeting NPM and the control shRNA pLKO.1 were obtained from The Open Biosystems Expression Arrest™TRC Library (Thermo Scientific, Rockford, IL, USA). The shRNA sequences are as follows: sh1 (TRCN0000062268): 5′-tttggacaacacattcttggc-3′, sh2 (TRCN0000062272): 5′-aatgtcttctacagaactagg-3′. For lentiviral infection, PLAT-F cells were seeded in 10-cm dishes, and transfected with 10 μg shRNA plasmids according to the protocol provided by Open Biosystems (Huntsville, AL, USA). The culture supernatants were collected 24 h after transfection. For viral infection, 2.0×10^5 of Ewing's sarcoma cells (NCR-EW2, RD-ES, and W-ES) were seeded in six-well plates, and incubated in the culture supernatant of PLAT-F transfectants with 8 μg/mL of polybrene for 24 h. To select the control pLKO.1 vector-positive (mock) or pLKO.1-shNPM-positive (sh1 or sh2) cells, 0.5 μg/mL puromycin (WAKO, Osaka, Japan) was added to the medium and cells were harvested after 5 days.

2.4 Quantitative RT-PCR (qRT-PCR)

The expression levels of RNA were measured using qRT-PCR. Briefly, total RNA was extracted using ISOGEN II reagent (Wako) according to the manufacturer's instructions. The cDNA was synthesized from total RNA using GoScript™ Reverse Transcription System (Promega, Madison, WI, USA). Reactions were performed using the TaqMan® GeneExpression Assay (Applied Biosystems, Foster City, CA, USA), the FastStart Universal Probe Master (Roche), and an Applied Biosystems 7300 Fast Real-Time PCR system (Applied Biosystems). Taqman probes employed were as follows: NPM1 (Hs02339479_g1) and ACTB (Hs03023943_g1). PCR was performed in triplicate, and the average expression levels were normalized to those of the *β-actin* gene.

2.5 Western blotting

Specific protein–protein interactions were confirmed by Western blotting. Briefly, protein samples were separated using SDS-PAGE and were subsequently transferred to PVDF membranes. Antibody reactions were performed using primary antibodies in conjunction with horseradish peroxidase-conjugated secondary antibodies (1:1000; GE Healthcare, Uppsala, Sweden). The primary antibodies were as follows: anti-NPM antibody (1:500, NA24, Santa Cruz, CA, USA), anti-ACTB antibody (1:1000, A5060, Sigma, St. Louis, MO, USA), anti-mouse IgG antibody (1:2000, NA931V, GE Healthcare), anti-rabbit IgG (1:2000, NA9340V, GE Healthcare), anti-Cyclin D1 antibody (1:500, A-12, Santa Cruz) and anti-NUCL antibody (1:500, MS-3, Santa Cruz). The immunocomplexes were detected using an enhanced chemiluminescence system (ECL Prime, GE Healthcare) and LAS-3000 (FUJIFILM, Tokyo, Japan).

2.6 2D-PAGE

For first dimension, the separation using isoelectric focusing (IEF), IPG dry strip gels (length 18 cm, p*I* range between 3.0 and 10.0, GE Healthcare) were rehydrated with rehydration buffer containing 30 μg of protein in Immobiline DryStrip Reswelling Tray (GE Healthcare). Proteins were separated according to their p*I* values at 26 kVh on a Multiphor II (GE Healthcare). After IEF, IPG gels were equilibrated with equilibration buffer for 20 min at room temperature. For separation in the second dimension, the equilibrated IPG dry strip gels were applied to 12% polyacrylamide gels and sealed with low-melting-temperature agarose (GE Healthcare). SDS-PAGE was performed at 200 V for 120 min (Biocraft, Japan, Tokyo).

2.7 Proliferation assay

To measure cell proliferation, 1.0×10^4 cells were placed in Nunclon Tissue Culture Dishes (T7432–2A, Nunclon, Roskilde, Denmark), and the number of cells in five defined areas (2 mm^2) was determined.

2.8 Immunoprecipitation

Transfected Ewing's sarcoma cells (1.0×10^7) were lysed with 2.1 mL lysis buffer containing 250 mM NaCl, 20 mM sodium phosphate (pH 7.0), 30 mM sodium pyrophosphate, 10 mM NaF, 0.10% NP-40, 5.0 mM DTT, 1.0 mM PMSF, and one Complete Protease Inhibitor Mixture Tablet™ (Roche, Brussels, Belgium). After centrifugation at 40 000 × *g* for 30 min, the supernatant was recovered, and 1.4 mL of water was added. The cell lysates were gently rotated at 4°C overnight, with 70 μL of anti-FLAG antibody-conjugated with agarose beads (Sigma). The beads were washed six times with a lysis buffer containing 150 mM NaCl, 12 mM sodium phosphate, 18 mM sodium pyrophosphate, 6.0 mM NaF, 0.06% NP-40, 3.0 mM DTT, and 0.60 mM PMSF. Precipitated proteins were eluted from the beads using 0.30 mg/mL FLAG peptide (Sigma) at 4°C for 2 h and concentrated by Vivaspin 0.5 mL Concentrator (VivaScience, Hannover, Germany).

2.9 Identification of proteins

Immunoprecipitated proteins were separated by SDS-PAGE using a gradient gel (Supersep TM Ace 191–15031, WAKO). To visualize total immunoprecipitated proteins, the gels were stained with 2-D-Silver Stain II "DAIICHI" (Daiichi Pure Chemicals, Tokyo, Japan). The separated proteins were extracted as peptides from the gels by in-gel digestion, as reported previously [24]. Briefly, the gels were cut into 24 pieces using a grid cutter (Gel Company, Tübingen, Germany). The gels were extensively washed with a solution containing acetonitrile and ammonium bicarbonate and treated with trypsin (Promega, Madison, WI) at 37°C overnight. The tryptic digests were recovered from the gel pieces, concentrated under vacuum, and resolubilized with 0.1% trifluoroacetic acid. The final trypsin digests were subjected to LC-MS/MS (Finnigan LTQ XL linear ion trap mass spectrometer, Thermo Electron, San Jose, CA, USA). A Mascot search (version 2.3.01; Matrix Science, London, UK) of the SWISS PROT database (*Homo sapiens*, 471 472 sequences in the Sprot_57.5 FASTA file) was conducted to identify proteins based on the mass of the peptide ion peaks. Proteins with Mascot scores ≥34 with at least two peptides were considered as positively identified. The search parameters were as follows: trypsin digestion allowing up to three missed tryptic cleavages; fixed modifications with carbamidomethyl; variable modifications of oxidation, acetylation and phosphorylation; 1^+, 2^+, and 3^+ peptide charge; peptide mass tolerance of 2.0 Da; and MS/MS tolerance of 1.0 Da for all tryptic-mass searches.

2.10 Statistical analysis

Microarray data sets (GSE17674) were downloaded from the Gene Expression Omnibus (http://www.ncbi.nlm.nih.gov/geo/). The performance of NPM binding proteins as prognostic factors was evaluated using receiver operator characteristic (ROC) analysis [25] as implemented in the R and Epi packages (Vienna R: A Language and Environment for Statistical Computing, http://www.R-project.org; Epi package for epidemiological analysis in R, http://staff.pubhealth.ku.dk/~bxc/Epi/). The Epi package was used to obtain the optimal cutoff score which maximized sensitivity, true positives/(true positives + false negatives) and specificity, and true negatives/(true negatives + false positives). The cutoff value was defined by comparing the value of gene expression of patients who experienced overall survival (OS) ≥ 3 years with those whose OS was <3 years according to published data [26]. The OS and disease-free survival (DFS) curves were calculated using the

